FEBS Letters 370 (1995) 46–52 FEBS 15864

The solution structure of the active domain of CAP18 — a lipopolysaccharide binding protein from rabbit leukocytes

Chinpan Chen[a], Roland Brock[a,**], Frederick Luh[a,***], Ping-Jung Chou[a], James W. Larrick[b], Rong-Fong Huang[a], Tai-huang Huang[a,*]

[a]*Division of Structural Biology, Institute of Biomedical Sciences, Academia Sinica, Nankang, Taipei 11529, Taiwan, ROC*
[b]*Palo Alto Institute of Molecular Medicine, Mountain View, CA 94043, USA*

Received 11 May 1995; revised version received 22 June 1995

Abstract We have employed the circular dichroism (CD) technique to characterize the solution structure of $CAP18_{106-137}$, a lipopolysaccharide (LPS) binding, antimicrobial protein, and its interaction with lipid A. Our results revealed that $CAP18_{106-137}$ may exist in at least three lipid A concentration-dependent, primarily helix conformations. The 'model' structure of $CAP18_{106-137}$ in 30% (v/v) TFE, determined by nuclear magnetic resonance (NMR) technique, was found to be a complete and very rigid helix. In this conformation, the cationic and hydrophobic groups of $CAP18_{106-137}$ are separated into patches and stripes in such a way that it can favorably interact with lipid A through either coulombic interaction with the diphosphoryl groups or hydrophobic interaction with the fatty acyl chains.

Key words: Lipid A; Antibacterial peptide; Endotoxin; NMR

1. Introduction

Endotoxins are lipopolysaccharides which form the main constituents of the outer leaflet of Gram-negative bacteria and perform vital functions. When librated they are potent mammalian toxins for mammalian cells, stimulating macrophages and endothelial cells to release inflammatory mediators such as tumor necrosis factor (TNF) and free radicals [1]. A rational approach to the control of inflammation caused by Gram-negative bacteria is to counteract the deleterious effects of LPS. One therapeutic approach is to identify proteins other than antibodies that bind to and neutralize LPS. Several such proteins have been identified, including *Limulus* anti-LPS factor (LALF) [2], human LPS binding protein (LBP) [3], bactericidal permeability increasing protein (BPI, CAP57) [4] and CAP18 [5]. Although many antimicrobial peptide structures have been determined, LALF is the only endotoxin binding protein to have had its 3D structure determined [6]. Furthermore, the structure of the LPS-binding protein/lipid A complex has remained elusive.

CAP18 is a lipopolysaccharide (LPS) binding protein first isolated from rabbit granulocytes [5]. Its amino acid sequence, deduced from cDNA clones, reveals a mature protein of 142 residues [7] which has no homology to known LPS binding proteins including CAP57/BPI, bacterial permeability increasing protein and other LPS binding proteins. The protein is composed of two domains: an N-terminal portion of unknown function and a C-terminal fragment of 37 amino acids ($CAP18_{106-142}$) that has LPS binding activity [8]. This fragment also has potent anti-microbial activity against both Gram-negative and Gram-positive bacteria [9]. A more potent fragment, $CAP18_{106-137}$, was identified by one of us [9] and used for the present studies. Recently a 21-amino acid peptide corresponding to residues 106–126 ($CAP18_{106-126}$) has been shown to have potent anti-Gram-positive and anti-Gram-negative bacterial activity [10]. Interestingly, the peptide mediates this activity via a remarkable permeabilizing effect on the inner membrane of *E. coli* [10]. The structure–function relationship of this peptide is still not clear. Here we report a combined CD and NMR study on the solution conformations of free and lipid A-bound $CAP18_{106-137}$ in various solvents. We show that indeed the peptide adapts a helical conformation when bound to lipid A isolated from *Salmonella minnesota* R595 strain.

2. Materials and methods

2.1. Materials

The amino acid sequence of $CAP18_{106-137}$ is shown below:

GLRKR LRKFR NKIKE KLKKI GQKIQ GLLPK LA

This peptide was synthesized with an Applied Biosystems model 430A or 431A peptide synthesizer and purified and characterized as described previously [8]. Lipid A (Refined Standard Endotoxin from *Salmonella minnesota* R595) was purchased from RIBI Imunochem Research Inc. (Hamilton, Montana, USA). Trifluoroethanol-d3 (TFE) was purchased from Cambridge Isotope (Woburn, MA, USA). Unless otherwise stated, all reagents and solvents were obtained commercially as reagent grade and used without further purification.

2.2. Circular dichroism

Lipid A stock solution (100 μM) was prepared by dissolving the appropriate amount of diphosphoryl lipid A in 1 mM sodium phosphate buffer, pH 7.0, containing 1 mM NaCl. The solution was swirled in a 60°C water bath for 30 s, then sonicated for 30 s. All CD experiments were carried out in 1 mM sodium phosphate buffer, pH 7.0, containing 1 mM NaCl and the appropriate amount of protein and TFE. CD experiments were carried out on a Jasco-J-720 CD spectrometer. Jasco Model 120-10 cylindrical quartz cell cuvettes with pathlengths of 1 or 10 mm were used. The parameters employed were: band width = 2 nm; slit width = sensitivity = 10 mdeg; response = 1 S; scan speed = 10 nm/min; scan width = 320–180 nm; step resolution = 0.5 nm. Temperature within the sample chamber was maintained at 28°C with a continuous nitrogen flow rate of 30–40 l/min. The absorbance spectrum was monitored while recording a CD spectrum to make sure enough light passed through the sample, especially at a wavelength below 200 nm. All spectra were an average of 4 scans, and processed by a J-720 noise reduction computer program. Reference spectra, obtained with samples containing all components except the protein, were

*Corresponding author. Fax. (886) (2) 785-3569.
E-mail: bmthh@ccvax.sinica.edu.tw

**Present address:* Vogtshaldenstrasse 5, 72074 Tübingen, Germany.

***Present address:* Department of Biochemistry, University of Cambridge, Tennis Court Road, Cambridge CB2 1QW, UK.

SSDI 0014-5793(95)00792-X

recorded after each spectrum and subtracted from the protein spectra. CD spectra were recorded in mDegree units. Conversion from mDegree to $\Delta\varepsilon$ was calibrated with (1S)-(+)-10-camphorsulfonic acid (CSA) by measuring the absorbance of CSA at 285 nm (absorption extinction coefficient = 34.5) and the CD spectrum at 290.5 nm (CD absorption coefficient = 2.36). The secondary structure was estimated from the CD spectra according to the method of Sreerama and Woody [11].

2.3. NMR experiments

Samples for NMR experiments were prepared by dissolving 3 mg of $CAP18_{106-137}$ in 0.35 ml of 50 mM phosphate buffer containing 30% TFE-d3, 60% H_2O and 10% D_2O. The pH of this sample was measured to be 3.5 (uncorrected). For amide proton exchange rate experiments the above NMR sample was lyophilized and redissolved in 30% TFE-d3/70% D_2O. All NMR spectra were obtained on a Bruker AMX600 spectrometer. All TOCSY (mixing time 80 ms with no trim pulse) and DQF COSY spectra were collected with 32 transients and 800 t_1 increments. All NOESY experiments (mixing times of 80, 100 and 300 ms) were collected with 48 transients and 700 t_1 increments. Spectra were recorded in TPPI mode. The spectral width was 7042 Hz. Water suppression was achieved by presaturation during recycle delay (1.4 S), and during the mixing time for the NOESY experiments. All data were processed on a Silicon graphic work station model 4D35/TG using Felix (Hare Research Inc.) or Bruker UXNMR programs. Prior to Fourier transformation of the free induction decays a skewed sine bell window function was applied to both dimensions. When quantitative measurements of cross-peak volumes were needed, 90°-shifted sine bells were applied in both dimensions. Data were zero-filled to 2K × 2K 'real' matrix with a digital resolution of 1.72 Hz/pt (Table 1).

3. Results and discussion

3.1. $CAP18_{106-137}$ – lipid A interaction

Fig. 1a shows the CD spectra of 20 μM $CAP18_{106-137}$, with the contribution from lipid A subtracted, in the presence of various amounts of lipid A. The helical contents estimated from these spectra show that in the absence of lipid A, $CAP18_{106-137}$ is in an unordered state. Addition of lipid A caused a increase in the formation of helical structure, as monitored by the depth of the two valleys at 207 nm and 220 nm and a peak at 192 nm in the CD spectra. Another prominent feature of these CD spectra is the lack of single isosbestic point for all curves. However, a single isosbestic point was observed when $CAP18_{106-137}$ was added stepwise to lipid A sample fixed at 20 μM concentration (Fig. 1b), suggesting that at fixed lipid A concentration the $CAP18_{106-137}$ molecule can exist in only two conformers, the bound helical form and the free random coil form. No change in the CD spectrum of free protein was observed when protein concentration was varied from 1 to 100 μM. The CD spectrum of lipid A is weak and noisy. Nevertheless, discernible change was detected in the concentration range of 25–35 μM. Thus, we attribute the lack of isosbestic point in Fig. 1a to structural changes, possibly multimer formation, in lipid A at higher concentration. Apparently, the structure of $CAP18_{106-137}$ bound to monomeric lipid A is different from that bound to polymeric lipid A complex. As a result, there exist at least three lipid A concentration-dependent protein conformers, an unordered conformer in the absence of lipid A, a highly helical conformer at high lipid A concentration, and an intermediate conformer(s) at intermediate lipid A concentration. The presence of an intermediate structure for $CAP18_{106-137}$ is further supported by the observation of non-monotonic change in the depth of the valley at 227 nm, as shown clearly in the CD

Table 1
^{1}H chemical shifts for $CAP18_{106-137}$ in 30% TFE at 302 K at pH 3.5, taking TMS resonance (0.00 ppm) as a reference

Residues	Chemical shift (ppm)				
	HN	Hα	Hβ	Hγ	Others
Gly[1]	–	4.06,3.91	–	–	–
Leu[2]	8.79	4.17	1.66,1.66	1.66	0.97,0.93
Arg[3]	8.58	4.01	1.96,1.90	1.78,1.71	δCH$_2$ 3.23,3.23 εNH 7.36
Lys[4]	8.17	4.05	1.88,1.88	1.57,1.43	δCH$_2$ 1.75,1.75 εCH$_2$ 3.02,3.02
Arg[5]	7.92	4.07	2.03,2.03	1.69,1.69	δCH$_2$ 3.16,3.16 εNH 7.25
Leu[6]	8.44	4.27	1.83,1.63	1.75	0.94,.0.89
Arg[7]	8.10	4.03	1.95,1.79	1.66,1.66	δCH$_2$ 3.21,3.21 εNH 7.36
Lys[8]	8.00	4.13	1.92,1.88	1.56,1.49	δCH$_2$ 1.70,1.70 εCH$_2$ 2.97,2.97
Phe[9]	8.33	4.37	3.28,3.28	–	2,6H 7.23, 3,5H 7.29, 4H 7.25
Arg[10]	8.59	3.88	1.96,1.87	1.65,1.65	δCH$_2$ 3.19,3.19 εNH 7.22
Asn[11]	8.13	4.51	2.99,2.87	–	NH$_2$ 7.62,6.92
Lys[12]	8.00	4.12	2.01,1.92	1.49,1.49	δCH$_2$ 1.71,1.60 εCH$_2$ 2.98,2.98
Ile[13]	8.00	3.70	1.90	1.35,1.00	γ_2 0.85, δ 0.65
Lys[14]	8.13	3.90	1.93,1.93	1.42,1.42	δCH$_2$ 1.71,1.71 εCH$_2$ 2.96,2.96
Glu[15]	7.94	4.06	2.28,2.19	2.62,2.51	–
Lys[16]	7.96	4.17	1.93,1.93	1.41,1.41	δCH$_2$ 1.77,1.77 εCH$_2$ 2.97,2.97
Leu[17]	8.54	4.10	1.89,1.48	1.65	0.85,0.85
Lys[18]	8.17	4.05	1.96,1.96	1.43,1.43	δCH$_2$ 1.70,1.61 εCH$_2$ 2.96,2.96
Lys[19]	7.83	4.14	2.07,1.95	1.51,1.51	δCH$_2$ 1.74,1.74 εCH$_2$ 3.00,3.00
Ile[20]	8.36	3.80	1.96	1.75,1.16	γ_2 0.95, δ 0.87
Gly[21]	8.44	3.90,3.79	–	–	–
Gln[22]	8.02	4.13	2.28,2.18	2.62,2.43	NH$_2$ 7.42,6.78
Lys[23]	7.94	4.19	2.01,2.01	1.58,1.48	δCH$_2$ 1.71,1.60 εCH$_2$ 2.94,2.94
Ile[24]	8.33	3.88	2.01	1.68,1.27	γ_2 0.94, δ 0.83
Gln[25]	8.13	4.02	2.20,2.18	2.55,2.43	NH$_2$ 7.17,6.64
Gly[26]	7.84	4.09,3.87	–	–	–
Leu[27]	7.84	4.44	1.85,1.68	1.79	0.92,0.90
Leu[28]	7.78	4.30	1.88,1.57	1.71	0.95,0.89
Pro[29]	–	4.35	2.37,1.83	2.12,1.99	3.78,3.56
Lys[30]	7.67	4.26	1.93,1.93	1.54,1.48	δCH$_2$ 1.71,1.71 εCH$_2$ 3.01,3.01
Leu[31]	7.90	4.27	1.72,1.57	1.71	0.90,0.87
Ala[32]	8.03	4.24	1.41	–	–

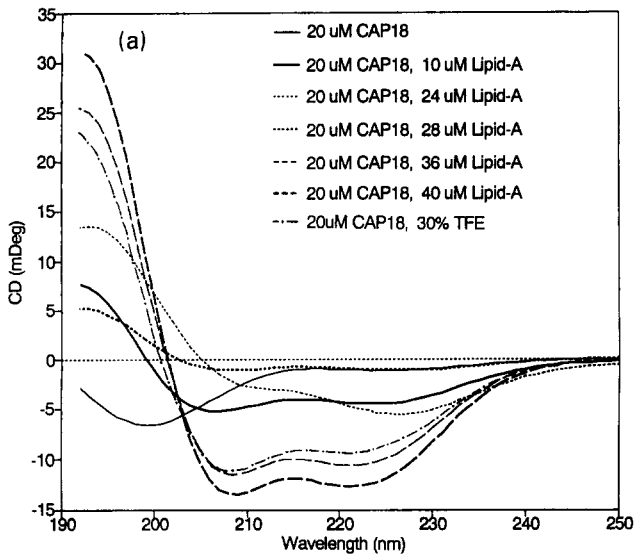

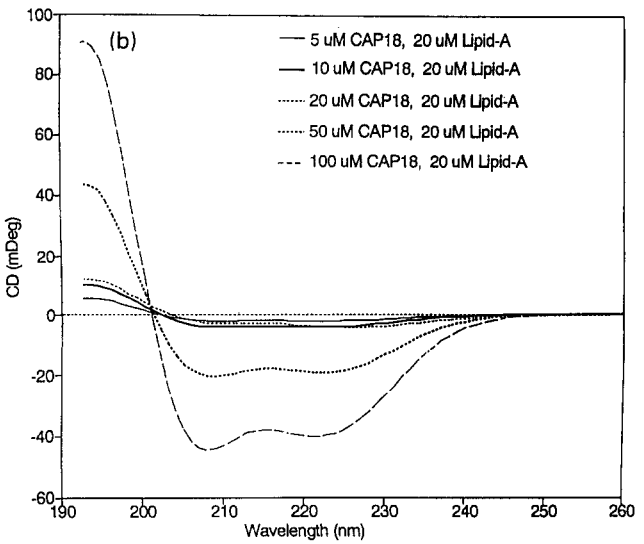

Fig. 1. (a) CD spectra of $CAP18_{106-137}$ in various lipid A concentrations. Samples employed for the present study contain 20 μM of $CAP18_{106-137}$ in 1 mM phosphate buffer, pH 7.0. Lipid A was prepared as described in the text. CD spectra were obtained at 28°C. (b) CD spectra of various concentrations of $CAP18_{106-137}$ in 20 μM of lipid A. All other conditions are the same as in Fig. 2a. A CD spectrum of 20 μM $CAP18_{106-137}$ in 30% (v/v) of TFE is also included in Fig. 1a.

spectrum of the sample with 24 μM lipid A. Transition between the two lipid A-bound coformers occurs at lipid A concentration around 20–35 μM.

3.2. NMR resonance assignments

In aqueous solution the proton spectrum of $CAP18_{106-137}$ showed a poor dispersion, characteristic of a random coil conformation. The 2D NOESY NMR spectrum of this sample showed no long range connectivity. Thus, free $CAP18_{106-137}$ in the absence of substrate is in an unordered structure, typical for most free peptides. Even though the CD spectra showed the presence of an ordered secondary structure in the presence of lipid A we were unable to determine the structure of $CAP18_{106-137}$/lipid A complex by NMR because of severe linewidth broadening when lipid A was added to the peptide solution. This suggests the formation of large aggregates of $CAP18_{106-137}$/lipid A complex under experimental conditions needed for NMR study. However, the CD spectrum of a 20 μM $CAP18_{106-137}$ in 30% (v/v) TFE is very similar to that observed with 20 μM $CAP18_{106-137}$ in 40 μM lipid A (Fig. 1a). Thus, we have determined the structure of $CAP18_{106-137}$ in 30% TFE. Although the similarily in CD spectra does not imply structural identity, using synthetic peptides or tryptic fragments it has been shown in several studies that only those peptides that adapt helical conformation in the native protein adopt helical conformation in the presence of TFE [12]. These results suggest that a peptide's propensity to form a helix is a prerequisite for the induction of an ordered helix by TFE.

We performed a complete series of two-dimensional NMR experiments to determine the structure of $CAP18_{106-137}$ in 30% TFE at three temperatures, 302K, 310K and 315K. Fig. 2 shows a representative 'fingerprint' region of a 2D TOCSY spectrum at 315K. Twenty-five $C_\alpha H$-NH scalar connectivities are clearly observed. Spectra obtained at different temperatures helped to resolve the spectral overlap and enabled us to assign all resonances. By following resonances at more than one temperature it was relatively straightforward to assign all the resonances using standard sequential resonance assignment strategy [13]. Four of the five single amino acids in the sequence were assigned first (F9, N11, P29 and A32). A32 was assigned from its unique COSY cross-peak between $C_\alpha H$ and $C_\delta H_3$. P29 was identified from TOCSY relayed cross-peaks $C_\alpha H$–$C_\delta H_2$. The two AMX spin systems of F9 and N11 were distinguished from the NOESY spectrum, based on the $C_\delta H_2$–$C_\beta H_2$ connectivities for F9. The two glycines (G21 and G26) were identified from their characteristic cross peaks in the 'fingerprint' region of the

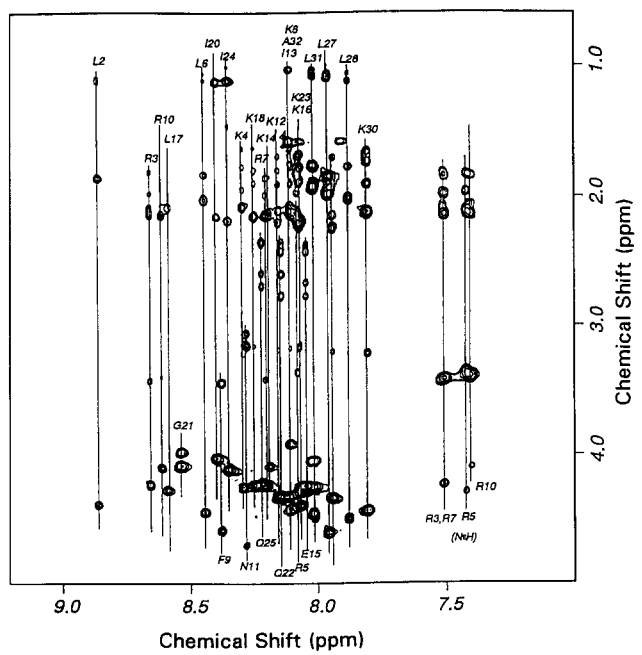

Fig. 2. Representative 2D TOCSY NMR spectrum of the 'fingerprint' region at 80 ms mixing time, showing the long range connectivities. Sample contains 2 mM $CAP18_{106-137}$ in 10 mM phosphate buffer, pH 3.5, in H_2O/D_2O/TFE = 60:10:30 (v/v/v) solvent at 315K. The assignments are also given on the spectrum.

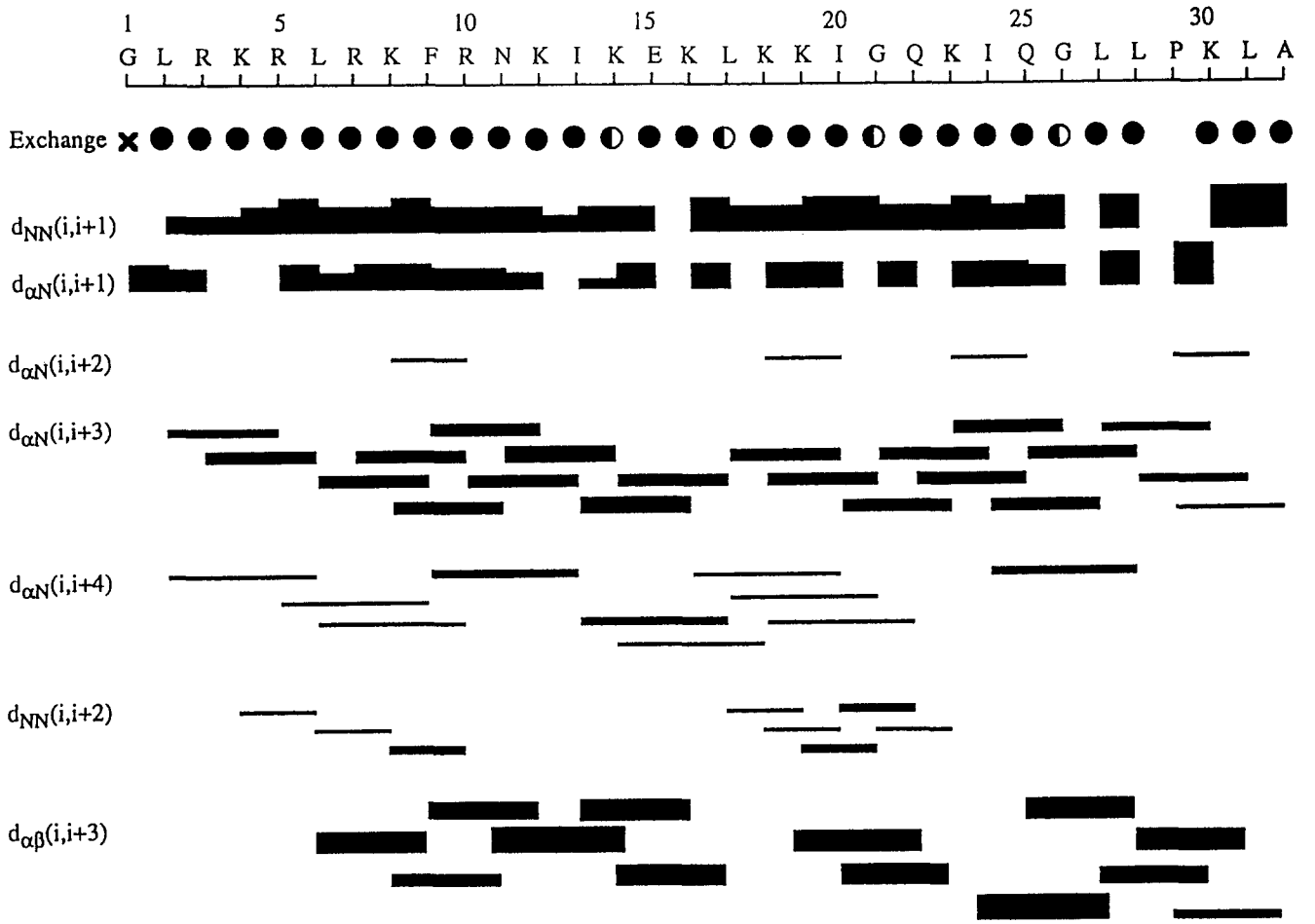

Fig. 3. Summary of the sequential connectivities and backbone amide proton exchange rates of $CAP18_{106-137}$. The bar thickness is proportional to the cross-peak intensity. Most of the amide protons, marked with filled circles, do not exchange over a period of several weeks. The exceptions are: (i) the amide proton of the N-terminal glycine, marked with an 'X', exchanges rapidly; (ii) the amide protons of four amino acids, marked with half-moon circles, lost 70–80% of their intensities in several days.

DQF-COSY spectrum. The spin systems of E15, Q22 and Q25 were identified from the TOCSY experiment where the remote connectivities, NH-βCH_2 were easily identified. The spin systems of the three Is and six Ls can be identified from the upfield region of the TOCSY and DQF-COSY spectra. The spin systems of Rs and Ks were assigned from the connectivity patterns of $C_\alpha H$-$C_\varepsilon H_2$ for arginine and $C_\alpha H$-$C_\varepsilon H_2$ for lysine. These assignments were reconfirmed from the cross-peaks between NH and side chain protons of Arg and Lys in the downfield region.

Sequential assignments were done on the basis of four sets of NOESY spectra at different temperatures and mixing times (80 ms mixing time at 296K, 100 and 300 ms at 302K, and 300 ms at 310K). Under these conditions most of the unresolved nOes were well-resolved. Although most of the assignments were straightforward, the weak sequential nOes of K12 NH to N11 $C_\alpha H$ and K14 NH to I13 $C_\alpha H$ were problematic. The $NH_i - NH_{i+1}$ nOes at different temperatures helped to resolve the confusion. The final assignments are listed in supplementary material.

3.3. Conformation of $CAP18_{106-137}$

Fig. 3 shows a summary of the nOe connectivities of backbone protons and the exchange rates of backbone amide protons at pH 3.5 in 30% TFE. The observation of several nOe cross-peaks, including those of NH_i–NH_{i+1}, $C_\alpha H_i$–NH_{i+1}, $C_\alpha H_i$–NH_{i+3}, $C_\alpha H_i$–$C_\beta H_{i+3}$, and $C_\alpha H_i$–NH_{i+2} nOes throughout the peptide is indicative of a molecule with a helix structure. The observation of weak $C_\alpha H_i - NH_{i+4}$ cross-peaks further suggests that it is an α-helix, rather than a 3_{10}-helix. Since only $C_\alpha H$(L28) – $C_\delta H_2$ (P29) nOe was observed, the proline-29 is likely to be in a *trans* conformation.

The cross-peak intensities of the 100 ms mixing time NOESY spectrum, obtained at 302K, were used to calculate the upper-boundary of the inter-proton distances. These distances were calibrated using a calibration curve based on the known distances of methylene protons and aromatic protons. According to this procedure the nOe peak intensities were assigned distances of 2–2.7 Å, 2–3.3 Å, 2.5–4.0 Å, and 3.0–5.0 Å depending on whether the cross-peak intensities were very strong, strong, medium or weak, respectively. Due to lack of stereospecific assignments, pseudoatoms were used whenever stereospecific protons were encountered [13]. From two-dimensional NOESY spectra obtained at different temperatures we obtained a total of 263 interproton restraints, including 90 inter-residue backbone proton restraints and 63 inter-residue sidechain proton restraints. Because of the intrinsic broad linewidth we did not use $^3J_{NH\alpha}$ to calculate torsional angle φ.

Three-dimensional structures of $CAP18_{106-137}$ were deduced

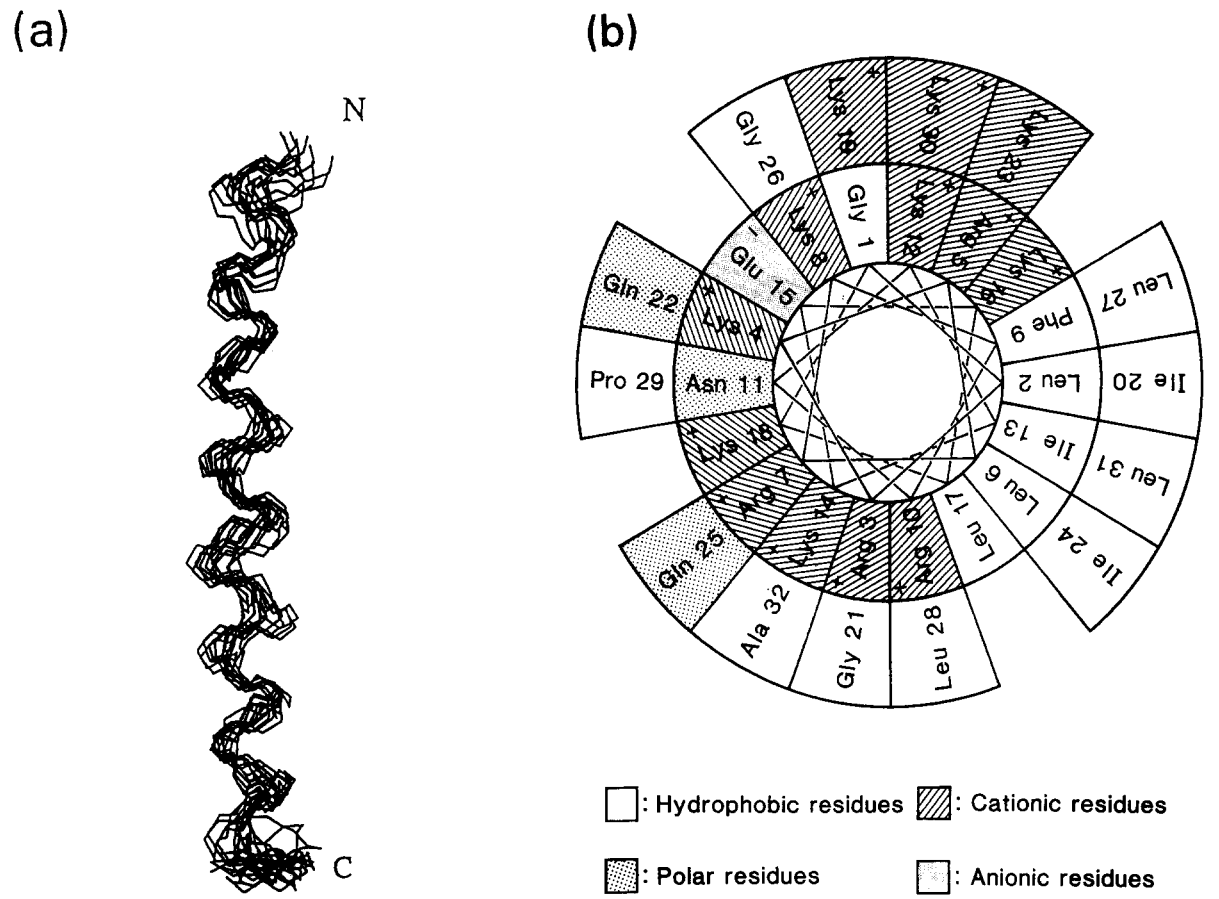

Fig. 4. (a) Superimposition of fifteen backbone structures of $CAP18_{106-137}$ deduced from 263 nOe constraints and refined with simulated annealing protocol in XPLOR program. The fifteen structures have the lowest overall energies and contain no single nOe violation greater than 0.3 Å. (b) Helical wheel plot of $CAP18_{106-137}$ showing the clustering of positively charged groups and the hydrophobic groups.

using the 263 nOe distance constraints by the dynamical simulated annealing method using the XPLOR program. The force field employed for structure calculation consists of only three terms: the covalent term which maintains correct bond lengths, angles, chiralities and planarities; the non-bonded interaction which is represented by the van der Waals repulsion term; and the nOe distance restraint term which is represented by a square-well potential. Three starting structures, α-helix, extended, and random coil, were employed to generate 300 structures. The violation in nOe constraints and the total energy of each structure were calculated. The computed structures were inspected on a Silicon Graphic workstation model 4D35/TG using the INSIGHT II program. Structures which contained too many nOe violations and had high final energies were discarded. Fifteen structures with no single nOe violation larger than 0.3 Å (average RMSD = 0.054 Å) and lowest energies were overlaid and are shown in Fig. 4a. The whole $CAP18_{106-137}$ molecule forms a nearly straight helix. We found that structures with larger bending have higher energy and more severe nOe violations. The coordinates of the structure has been deposited in Brookhaven Protein Data Bank (Identification number 1LYP).

3.4. Stability of the helix

The stability of the helix can be deduced from the exchange rate of the amide protons, i.e. the rate of decrease in intensities when the solvent was changed from H_2O to D_2O in the 2D TOCSY spectra, the results for which are shown in Fig. 3. The intensity of most amide protons did not change after several days in D_2O, with the exception of the intensities of the K14, L17, G21 and G26 residues which decreased 70–80% in the same time period. Thus the helix is extremely stable even at those few more flexible sites. The stability of the helix is further demonstrated in the high melting temperature of the peptide, as indicated by the presence of sharp exchangeable amide proton resonances at a temperature as high as 77°C (figure not shown). Using the aromatic proton resonances between 7.5 ppm and 8.0 ppm as references, we estimate that roughly 50% of the amide proton intensity is still observable at 77°C.

3.5. State of lipid A

Lipid A is an amphipathic molecule possessing a charged diphosphoryl glucosamine head group and up to seven hydrophobic fatty acid chains [1]. At present, the details of the mechanism underlying the interaction of lipid A with host cell membranes or with particular components of the membranes leading to well-known biological effects are not well understood. All available data suggest that full endotoxic activity is expressed by a molecule containing two (D-*gluco*-configurated) hexosamine residues, two phosphoryl groups, and six saturated fatty acids including 3-acyloxylated groups with a defined chain length and in a distinct location. Whether the endotoxic confor-

mation relates to a single endotoxin molecule or to a peculiar aggregation state remains to be elucidated. Evidence also has been provided that a highly disaggregated form of Re-LPS (possibly the monomer) may function as the active unit [14].

Our observation of the drastic broadening of the proton NMR resonances of the $CAP18_{106-137}$ with no observable precipitate formation when lipid A was added to the protein sample suggests that under the experimental conditions for NMR at millimolar concentration the lipid A molecules exist in large aggregated structures, not in monomeric or other lower order forms. On the other hand, at the micromolar concentration range employed for our CD study, lipid A appears to form more than one kind of complex with $CAP18_{106-137}$. This is indicated by the lack of an isosbestic point for the CD spectra of $CAP18_{106-137}$ when lipid A was added stepwise, and the observation of an isosbestic point at fixed lipid A concentration. While it is tempting to fit the helical content curve to obtain binding parameters, the lack of information on binding stoichiometry, number of species involved and the intrinsic uncertainty associated with estimating the helical content from CD curves make such an exercise much too speculative at present.

3.6. *Structure of $CAP18_{106-137}$ in lipid A complex*

No NMR or crystal structure of protein or peptide complex with lipid A has been published to date. Studies on the interaction of small peptides, including polymyxin B, with lipid A confirmed that multiple structural factors are responsible for optimal binding of the peptide to lipid A, including the amphipathic and cationic features of the primary amino acid sequence, the hydrophobicity, the size of the structure and the peptide conformation [15]. From the X-ray crystal structure of the LPS binding protein, LALF an amphipathic loop was proposed as the LPS binding motif [6]. This loop is distinguished by an alternating series of positively charged and hydrophobic residues that, by virtue of the extended β-conformation, point in opposite directions, and a single pair of positive charges that, because of the β-turn conformation, point in the same direction and maintain the amphipathicity. Similar structures have been proposed for two other mammalian LPS binding proteins, LBP [16] and BPI [17]. The present CD work is the first to show that indeed $CAP18_{106-137}$ adapts a helical conformation when bound to lipid A. The 'model' structure of $CAP18_{106-137}$ in 30% (v/v) TFE determined by NMR further revealed that the helix spans the whole molecule and is very rigid. However, it should be pointed out that since $CAP18_{106-137}$ can assume different structures at different lipid A concentration the structure determined in TFE is probably better resembles that observed in high lipid A concentration. Our result is consistent with previous observations that peptides with higher helical propensity also possess higher antimicrobial activity [10]. Our observation of a complete helical structure for $CAP18_{106-137}$ is in contrast to that of LALF but is similar to that of many membrane peptides [17] including melittin [18], magnin 2 [19], and cercropins [20]. In comparison with melittin, $CAP18_{106-137}$ is much more hydrophilic. From the helical wheel projection of the peptide shown in Fig. 4b we found patches of positively charged residues including 11 of the first 19 residues near the N-terminus. These positively charged groups span an angle of 260°. For residues near the C-terminus, residues 20–32 there are 9 hydrophobic residues spanning an angle of over 220°. For the whole molecule the hydrophobic residues span an angle of about 100°. Such a special arrangement of the amino acid residues renders it equally favorable for the $CAP18_{106-137}$ molecule to bind to either the negatively charged diphosphoryl groups or the hydrophobic fatty acyl chains. Preliminary computer modeling showed that the positively charged groups are separated by distances optimal for interaction with the two negatively charged diphosphoryl groups at 10.9 Å apart. We hypothesize that the major impetus for forming the helix structure is to form charged or hydrophobic patches and stripes, thus explaining the observation that variants of the 20-residue peptide corresponding to residues 106–125 of CAP18, $CAP18_{106-125}$, with higher helical propensity are also more potent antimicrobial agents [10].

Other hints on the mechanism of the interaction between $CAP18_{106-137}$ and lipid A can be found from comparing the activity of various CAP18 peptides with different lengths and mutations. Among the published CAP18 peptides $CAP18_{106-137}$ appears to be the most potent antimicrobial peptide, with an IC_{50} of 20 nM against *Salmonella minnesota* R595 strain [9], higher than $CAP18_{106-125}$ and its variants [10]. This suggests that the additional interaction due to the C-terminus hydrophobic residues in $CAP18_{106-137}$ plays a major role in CAP18 binding to lipid A. Replacing the two positively charged residues, Arg-5 and Lys-16, with alanine, which has high helix propensity and is hydrophobic, resulted in increased antibacterial activity and faster kinetics of permeabilization. This finding further indicates the importance of hydrophobic interaction and the helical conformation.

Acknowledgments: This work is supported by a grant from the National Science Council of the Republic of China (NSC83-0203-B001-102). We thank Mr. Jen-Ning Yang for performing CD spectral calibration.

References

[1] Rietschel, E.T., Kirikae, T., Schade, F.U., Mamat, U., Schmidt, G., Loppnow, H., Ulmer, A.J.,Zähringer, U., Seydel, U., Padova, F.D., Schreier, M. and Brade, H. (1994) FASEB J. 8, 217–225.
[2] Akitagawa, J., Miyata, T., Ohtsubo, S., Nakamura, T., Morita, T. Takeo, T. and Shimonishi, Y. (1986) J. Biol. Chem. 261, 7357.
[3] Tobias, P., Mathison, J., and Ulevitch, R. (1988a) Annu. Rev. Med. 38, 417–432.
[4] Farley, M.M., Shafer, W.M. and Spitznagel, J.K. (1987) Infect. Immunol. 55, 1536.
[5] Hirata, M., Yoshida, M., Inada, K. and Kirkae, T. (1988) Poster Presentation, 3rd International Endotoxin Conference, Amsterdam, The Netherlands.
[6] Hoess, A., Watson, S., Siber, G.R. and Liddington, R. (1993) EMBO J. 12, 3351–3356.
[7] Larrick, J.W., Morgan, J.G., Palings, I., Hirata, M. and Yen, M.H. (1991) Biochem. Biophys. Res. Commun. 179, 170–175.
[8] Larrick, J.W., Hirata, M., Zheng, H., Zhong, J. Bolin, D., Cavaillon, J.-M., Warren, H.S. and Wright, S.C. (1994) J. Immunol. 152, 231–240.
[9] Larrick, J.W., Hirata, M., Shimomoura, Y., Yoshida, M., Zheng, H., Zhong, J. and Wright, S.C. (1993) Antimicrob. Agents Chemother. 37, 2534–2539.
[10] Tossi, A., Scocchi, M., Skerlavaj, B., Gennaro, R. (1994) FEBS Lett. 339, 108–112.
[11] Sreerama, N. and Woody, R.W. (1993) Anal. Biochem. 209, 32–44.
[12] Dyson, H.J., Sayre, J.R., Merutka, G., Shin, H.-C., Lerner, R.A. and Wright, P.E. (1992) J. Mol. Biol. 226, 819–835.
[13] Wüthrich, K. (1986) in: NMR of Proteins and Nucleic Acids, Wiley Intersciences, New York.
[14] Takayama, K., Din, Z.Z., Mukerjee, P., Kook, P.H. and Kirkland, T.N. (1990) J. Biol. Chem. 265, 14023–14029.

[15] Rustici, A., Velucchi, M., Faggioni, R., Sironi, M., Gehzzi, P., Quataert, S., Green, B. and Porro, M. (1993) Science 259, 361–365.
[16] David, S., Mathan, V.I. and Balaram, P. (1992) Biochim. Biophys. Acta 1123, 269–274.
[17] Saberwal, G. and Nagaraj, R. (1994) Biochim. Biophys. Acta 1197, 109–131.
[18] Terwilliger, T.C. and Eisenberg, D. (1982a) J. Biol. Chem. 257, 6010–6015.
[19] Marion, D., Zasloff, M., and Bax, A. (1988) FEBS Lett. 227, 21–26.
[20] Sipos, D. Andersson, M. and Ehrenberg, A. (1992) Eur. J. Biochem. 209, 163–169.